ACS OMEGA

http://pubs.acs.org/journal/acsodf

Article

Kinetic Study of Waste Tire Pyrolysis Using Thermogravimetric Analysis

Aida M. Ramírez Arias, Juan Carlos Moreno-Piraján,* and Liliana Giraldo

Cite This: *ACS Omega* 2022, 7, 16298−16305

Read Online

ACCESS | Metrics & More | Article Recommendations | Supporting Information

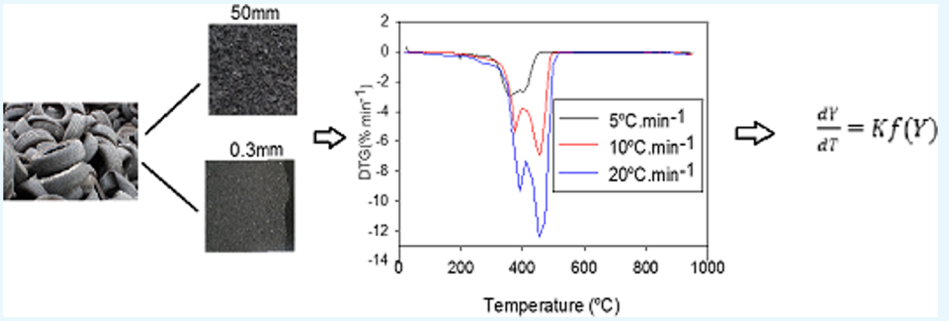

ABSTRACT: The influence of particle size (0.3 and 5.0 mm) and heating rate (5, 10, and 20 °C min^{-1}) on the kinetic parameters of pyrolysis of waste tire was studied by thermogravimetric analysis and mathematical modeling. Kinetic parameters were determined using the Friedman model, the Coats−Redfern model, and the ASTM E1641 standard based on Arrhenius linearization. In the Friedman model, the activation energy was between 40 and 117 kJ mol^{-1} for a particle size of 0.3 mm and between 23 and 119 kJ mol^{-1} for a particle size of 5.0 mm. In the Coats−Redfern model, the activation energy is in a range of 46 to 87 kJ mol^{-1} for a particle size of 0.3 mm and in a range of 43 to 124 kJ mol^{-1} for a particle size of 5.0 mm. Finally, in the ASTM E1641 standard, the activation energy calculated was between 56 and 60 kJ mol^{-1} for both particle sizes. This study was performed to obtain kinetic parameters from different mathematical methods, examining how the particle size and heating rate influence them.

INTRODUCTION

Worldwide, approximately 4.4 million tons of tires are generated per year, of which only 2% is recycled.[1] The remaining 98% ends up in warehouses, and if there is no adequate waste management it affects human health due to proliferation of pests causing diseases such as dengue and malaria, among others.[2,3] As it is a non-biodegradable material, it is necessary to act against this environmental problem.[4,5] Currently, incineration is the most used treatment for waste tire management, reducing the total volume of the landfill by 90%. However, these procedures contribute to environmental pollution because of the generation of polychlorinated dibenzofurans and polychlorinated dibenzodioxins.[4,6,7] For this reason, it is vital to find alternatives to manage waste tires without increasing the environmental contamination. The most viable process is using waste tires to obtain new materials from pyrolysis, such as activated carbon. In literature, yields have been found between 33 and 40% w w^{-1}.[8,9] This percentage varies depending on the composition of the tire and the pyrolysis conditions. Tires are composed of volatile matter, rubber, textiles, sulfur, steel, and metals. Rubber is obtained after subjecting the tires to crushing and demolding the steel. It is composed of natural rubber (NR), synthetic rubber [which is composed of butadiene (BR) and butadiene styrene (BSR)], and dyes. When rubber is subjected to pyrolysis, it produces three product fractions: solids (char), liquids (oil), and gases (gas). The percentage of solids is 33−38% w w^{-1}; for liquids, it is 38−55% w w^{-1}; and for gases, it is 10−30% w w^{-1}.[4,10] In the pyrolysis process, the kinetic study is essential to optimize the process parameters and obtain byproducts. Pyrolysis kinetics thermogravimetrically measures the weight loss as a function of time and temperature.[11,12] The heat and mass transfer between the sample, the sample holder, and the carrier gas can be considered negligible at controlled conditions. Therefore, the heat and mass changes are attributed to the chemical kinetic process rather than other processes.[13,14] With thermogravimetric analysis (TGA) and differential thermogravimetry (DTG), different kinetic models have been developed to study the pyrolysis mechanism and its kinetic parameters, such as the activation energy, rate constant, reaction order, and pre-exponential factor.[2,15−18] Different

Received: November 10, 2021
Accepted: March 16, 2022
Published: May 2, 2022

https://doi.org/10.1021/acsomega.1c06345
ACS Omega 2022, 7, 16298−16305

studies of tire pyrolysis have been found in literature. Miranda et al.[19] studied the possible routes for the pyrolysis reaction mechanism in batch reactors, finding that the reaction temperature influences the pyrolysis reaction mechanism of the waste tire and that the reaction order could not be 1. Leung and Wang[20] studied the thermal decomposition of scrap tires using non-isothermal TG methods at 20−600 °C temperature, different heating rates, and powder sizes. These authors concluded that the heating rate significantly affects tire pyrolysis while the tire powder size presents no significant effect. A three-component simulation model was considered to degrade different tire materials. Additionally, they found that the heating rate significantly affects the performance of tire pyrolysis. They applied a three-component simulation model, finding values of 54, 148, and 165 kJ mol^{-1} for the activation energy and 2.3×10^3, 1.5×10^{10}, and 3.5×10^{10} min^{-1} for the collision factor. Yaxin and Bingtao[21] carried out studies with tire dust at a temperature between 600 and 800 °C, finding two stages of thermal degradation with activation energies between 137.4 and 176 kJ mol^{-1} and 2.0×10^8 and 4.7×10^{12} min^{-1} as the collision factor. Boyu et al.[22] studied the formation of isoprene and DL-limonene during the pyrolysis of waste tire using the Kissinger and Friedman method, where significant differences were found in the kinetic parameters in each model with activation energies between 113 and 155 kJ mol^{-1}. Mkhize et al.[23] investigated the pyrolysis kinetics of waste tires in three cases (no catalyst, ZSM-5, and MnO_2) at different heating rates, using the Friedman and Kissinger method. Finding no apparent difference between the devolatilization processes of waste tires without a catalyst and with ZSM-5 and with MnO_2, there is a positive influence on the thermal decomposition of waste tires. Menares et al.[24] studied the fast pyrolysis of waste tires by quasi-isothermal TGA, kinetic modeling, and analytical pyrolysis coupled with gas chromatography/mass spectrometry (Py-GC/MS). The TGA demonstrated that the pyrolysis of waste tire is governed by devolatilization, condensation, and depolymerization reactions up to 482 °C. At higher temperatures, cyclization and aromatization of the primary products take place to form mainly monoaromatics. The E_a values calculated by the Starink model ranged between 101.5 and 176.7 kJ mol^{-1}, while the model-based kinetics was 152.7 kJ mol^{-1}. This research aims to study the pyrolysis kinetics of waste tires using different particle sizes, heating rates, and three mathematical methods. Despite several pyrolysis studies having been reported previously, the effects of the three mathematical methods used (Friedman, Coats−Redfern, and ASTM E1641), the heating rate, and the particle size on tire pyrolysis have not been addressed with a kinetic approach. For this reason, the kinetic parameters of waste tire pyrolysis were determined using TGA with the Hitachi equipment, TGA/STA7200, at a flow rate of 50 mL min^{-1} of N_2 with two rubber particle sizes (3 and 5.0 mm) and three heating speeds (5, 10, and 20 °C min^{-1}).

METHODS

Waste Tire Treatment. The waste tire was obtained from a tire collection company. First, the waste tires were cleaned with pressurized air to remove dust on the surface. Subsequently, the tires were cut in a knife mill to obtain two particle sizes, 0.3 mm, and 5.0 mm. After that, the steel after grinding was removed with a magnetic medium so that only the tire's rubber remains.

Waste Tire Pyrolysis. Approximately 10 mg of tire rubber was weighed to different particle sizes (0.3 and 5.0 mm) using a Hitachi High-Tech Sciences TGA/STA7200 instrument. First, pyrolysis was carried out at room temperature from 18 to 900 °C using nitrogen as a reaction gas at a flow rate of 50 mL min^{-1}, before starting the experiment, a nitrogen flow was passed for 15 min. Then, three heating rates (5, 10, and 20 °C min^{-1}) were used to degrade the waste tire at two particle sizes gradually.

Proximal Analysis. Using the TG technique, the proximal study considers the ASTM D-7582-15 standard. Humidity, volatile matter, ashes, and fixed carbon were determined.

Elemental Analysis. The contents of carbon (C), hydrogen (H), nitrogen (N), and sulfur were determined using Thermo Scientific FLASH 2000 Organic equipment, an elemental analyzer with Eager Smart data handling software. For this, the mass of the sample is weighed and heated to 950 °C, adding 300 mL of oxygen at a purity of 99.995%.

Kinetic Analysis. To determine the kinetic parameters, among them, activation energy (E_a), kinetic constant (K), reaction order (n), and collision factor (A), the results were obtained in the TGA using the mathematical models of Coats−Redfern, Friedman, and ASTM E1641.

In general, for the process

$$aA_{(solid)} \rightarrow bB_{(solid)} + cC_{(gas)}$$

The formal kinetic expression can describe the consumption of component A as eqs 3 and 5.

Friedman Differential Method. The change in mass used to study the kinetics of decomposition is expressed in terms of the mass conversion factor (Y)[25]

$$Y = \frac{m_0 - m_t}{m_0 - m_f} \tag{1}$$

where m_0 is the initial mass, m_t mass in a specific time, and m_f final mass after the process. The thermal decomposition of solids is defined by the conversion rate ($dY \cdot dT^{-1}$) by the expression

$$\frac{dY}{dT} = K(T)f(Y) \tag{2}$$

where $K(T)$ is the temperature-dependent rate constant and $f(Y)$ is an algebraic function that depends on the mechanism that controls the rate of the process. Arrhenius eq 3 expresses the reaction rate

$$K(T) = A\, e^{(-E_a/RT)} \tag{3}$$

where A is the pre-exponential factor (min^{-1}), (E_a) is the apparent activation energy (kJ mol^{-1}), T is the absolute temperature in (K), and R is the gas constant 8.314×10^{-3} kJ K^{-1} mol^{-1}.

Therefore, $f(Y)$ is independent of temperature and dependent on the degree of progress (Y) is

$$f(Y) = (1 - Y)^n \tag{4}$$

Substituting eqs 3 and 4 in eq 2, it is obtained

$$\frac{dY}{dT} = A\, e^{(-E_a/RT)}(1 - Y)^n \tag{5}$$

In eq 5, applying the logarithm

https://doi.org/10.1021/acsomega.1c06345
ACS Omega 2022, 7, 16298−16305

$$\ln\left(\frac{dY}{dT}\right) = \ln A - \frac{E_a}{RT} + n\ \ln(1 - Y) \tag{6}$$

Substituting eq 1 in eq 6

$$\ln\left(\frac{dY}{dT}\right) = \ln A - \frac{E_a}{RT} + n\ \ln\left(\frac{m_t - m_f}{m_0 - m_f}\right) \tag{7}$$

At different heating rates ($dY{\cdot}dT^{-1}$), the temperature required to achieve the same conversion (Y) varies for each sample; for this reason, the activation energy using a linear regression $\ln(dY{\cdot}dT^{-1})$ versus $(1{\cdot}T^{-1})$ for a constant value of Y is determined where the slope $m = -E_a{\cdot}R^{-1}$. Subsequently, using the activation energy found above, another linear regression of $[\ln(dY{\cdot}dT^{-1}) + E_a{\cdot}R^{-1}{\cdot}T]$ versus $\ln(1 - Y)$, the slope corresponds to n (reaction order), and the intersect is the pre-exponential factor.

Coats–Redfern Integral Method.[26] According to Redhead,[27] at a maximum pyrolysis temperature eq 8

$$\left(\frac{d^2Y}{dT^2}\right) = 0 \tag{8}$$

The kinetic equation of the decomposition of a solid is defined in eq 9

$$\left(\frac{dY}{dt}\right) = K(1 - Y)^n \tag{9}$$

where t is the reaction time, K is the equilibrium constant, and n is the reaction order. K is defined as in eq 3, replacing eq 3 in eq 9, it is obtained

$$\left(\frac{dY}{dt}\right) = A\ e^{(-E_a/RT)}(1 - Y)^n \tag{10}$$

By expressing eq 10 as a function of the heating rate, where $T = T_i + Bt$, B is the heating rate in ($k\ min^{-1}$), you get

$$\left(\frac{dY}{dt}\right) = \left(B\frac{dY}{dT}\right) = A\ e^{(-E_a/RT)}(1 - Y)^n \tag{11}$$

Applying eq 7

$$\left(\frac{d^2Y}{dT^2}\right) = \frac{d\left(-B\frac{dY}{dT}\right)}{dT} = 0 \tag{12}$$

By replacing, it is obtained
Substituting eq 11 in eq 12, we have

$$\left(\frac{d^2Y}{dT^2}\right) = \frac{d(-A\ e^{(-E_a/RT)}(1 - Y)^n)}{dT} = 0 \tag{13}$$

Applying the derivate in eq 13

$$\mathrm{Ln}\left(\frac{B}{T_f^2(1 - Y_f)^{n-1}}\right) = \mathrm{Ln}\frac{nAR}{BE_a} - \frac{E_a}{RT_f} \tag{14}$$

where T_f is the temperature at the maximum rate and Y_f is the conversion to the maximum reaction rate used. To simplify, we define $n = 1$, therefore

$$\mathrm{Ln}\left(\frac{B}{T_f^2}\right) = \mathrm{Ln}\frac{AR}{BE_a} - \frac{E_a}{RT_f} \tag{15}$$

Using a linear regression of $\mathrm{Ln}(B{\cdot}T_f^2)$ versus $(1{\cdot}T_f^{-1})$, where with the slope $m = -E_a{\cdot}R^{-1}$, the activation energy is determined, and the intersection is $\mathrm{Ln}(AR{\cdot}BE_a^{-1})$ defined with this the pre-exponential factor.

Standard Test Method, ASTM E1641. In this case, the kinetic study is performed using the standard test method for decomposition kinetics by thermogravimetry, ASTM 1641. To determine the kinetic energy, eqs 16 and 17 are used, the slope is (K) corresponding to $\Delta(\log\beta)/\Delta(1/T)$ and b corresponds to 0.457 K^{-1} for the first iteration. Additionally, E is the activation energy ($J\ mol^{-1}$), A is the pre-exponential factor, β is the heating rate, and A, eq 17, is the value of an integral approximation taken from ASTME 1641 for the refined value of $E(RT_c)^{-1}$, where T_c is the temperature at constant conversion for the heating rate closest to the midpoint of the experimental heating rates, eq 16.

$$E = -\left(\frac{R}{b}\right) \times [\Delta(\log\beta)/\Delta(1/T)] \tag{16}$$

To determine the pre-exponential factor and the kinetic constant, eqs 17 and 18 are used. Where α is the percentage at which temperatures (95%) and β velocity closest at the midpoint of heating

$$A = -(\beta'/E) \times R \times \ln(1 - \alpha) \times 10^a \tag{17}$$

$$k = A \times e^{-(E_a/RT)} \tag{18}$$

In ASTM 1641, $E_a{\cdot}(RT_c)^{-1}{\cdot}T$, where T_c it is the constant conversion temperature for the heating rate at the midpoint of experimental heating rates, and the temperature is taken at 95% weight loss.

RESULTS AND DISCUSSION

Proximal analysis of the waste tire (Table 1) is performed. The highest composition percent corresponds to the volatiles, 62.37%, such as colorants; fixed carbon, 30.34%; humidity, 0.66%; and ash, 6.63%. Ash is an inorganic material, such as zinc, nickel, and iron. The composition of waste tire depends on the manufacturer and the kind of tire (and the type of vehicle), therefore leading to different results. In elemental analysis, the highest composition percentage is carbon (C) 81.44%, followed by hydrogen (H) 8.19%, oxygen (O) 5.86%, nitrogen (N) 3.00%, and finally sulfur (S) 1.5% added during the tire vulcanization process.

Table 1. Characterization of Waste Tires by Proximal Analysis and Elemental Analyses

proximal analysis		elemental analysis	
humidity	0.66%	carbon	81.44%
volatiles	62.37%	hydrogen	8.19%
ash	6.63%	nitrogen	3.00%
fixed carbon	30.34%	oxygen	5.86%
		sulfur	1.50%

The waste tire, according to its general kinetic decomposition, is defined as

$$E_a(RT_c)^{-1}$$

According to previous studies, the elemental composition of the waste rubber is NR, butadiene rubber (BR), butadiene–styrene rubber (BSR), and additives, such as carbon black, zinc oxide, and sulfur.[19] In this study, the differential model, the integral model, and the standard test method ASTM E1641 are

https://doi.org/10.1021/acsomega.1c06345
ACS Omega 2022, 7, 16298−16305

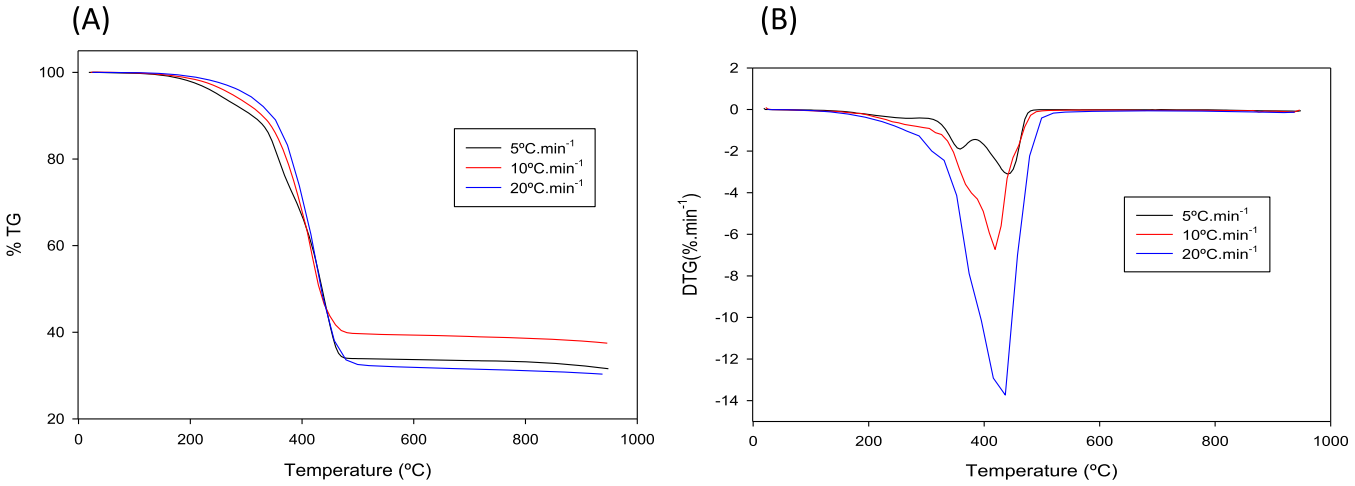

Figure 1. (A) TGA and (B) DTG with a nitrogen flow rate of 50 mL min^{-1} for the waste tire with a particle size of 0.3 mm.

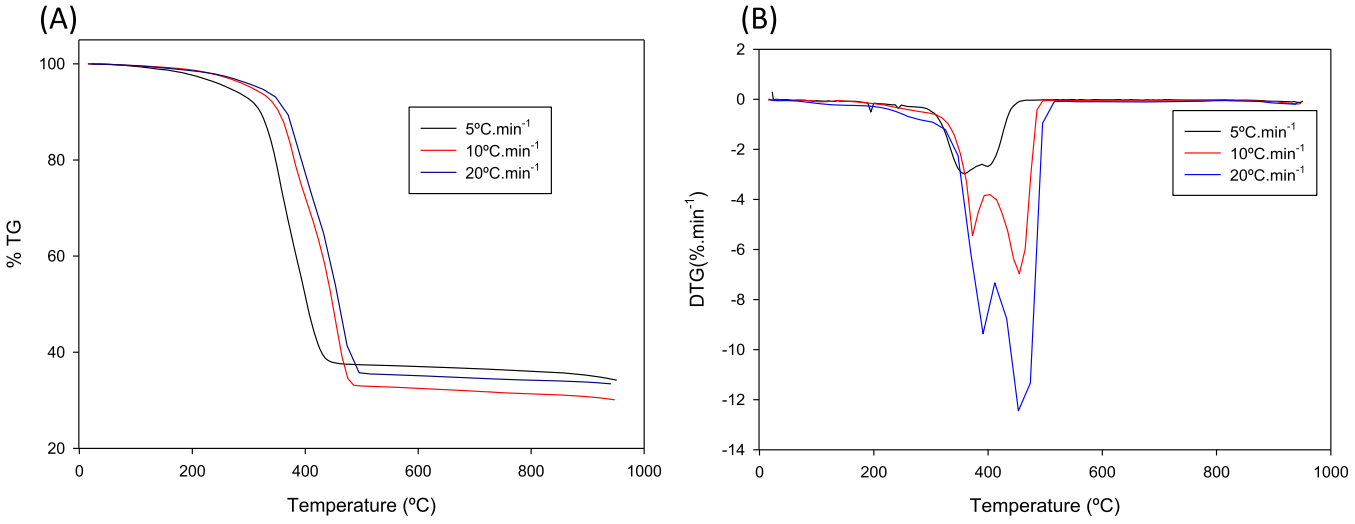

Figure 2. (A) TGA and (B) DTG with a nitrogen flow rate of 50 mL min^{-1} for the waste tire with a particle size of 5.0 mm.

used to determine the kinetic parameters, such as the activation energy, kinetic rate constant, and collision factor. For the determination of these kinetic parameters, it is assumed that:

1. All reactions are of first-order $n = 1$.
2. Carbon black is inert at the temperatures used.
3. The main polymeric components such as NR, butadiene rubber (BR), and butadiene−styrene rubber (BSR) do not contribute significantly to the formation of carbon and become almost entirely volatile during pyrolysis.[28−31]

Figures 1 and 2 show that the observed sample changed with increasing temperature, whether physical or chemical. Considering the three different heating rates of 5, 10, and 20 °C min^{-1}, for a particle size of 0.3 mm (Figure 1A) at a heating rate of 5 °C min^{-1}, the highest percentage of mass loss is observed to occur between 200 and 500 °C. As a result of exothermic behavior. For a heating rate of 10 °C min^{-1}, the highest mass loss occurs between 200 and 520 °C. Finally, for a heating rate of 20 °C min^{-1}, the highest mass loss is between 200 and 550 °C. There is a shift in the decomposition range toward higher temperatures as the heating rate increases, which indicates more energy and achieves the exact conversion. For the 5.0 mm particle size (Figure 1B), the highest percentage of mass is found in a range from 220 to 420 °C for a rate of 5 °C min^{-1}. It is between 220 and 500 °C for a heating rate of 10 °C min^{-1}, and finally for a heating rate of 20 °C min^{-1} in a range between 220 and 510 °C. This shows the same behavior as observed for the 0.3 mm particle size, a shift to the right with increasing heating rate as a higher temperature provides energy that facilitates heat transfer in the surrounding areas and the system. Additionally, when comparing Figures 1 and 2 at the same heating rate but different particle sizes, no significant variations are evidenced in the percentage of mass loss. However, a larger particle size causes more significant temperature gradients within the particle. Nevertheless, the particle sizes used here did not influence the speed of the process because the TG curves are superimposable. These results agree with what was reported in previous studies, where particle sizes less than 5.0 mm do not influence the speed of the process. It should be noted that in addition to intraparticle transport, which is affected by the size of the particles, the global velocity can also be influenced by two more parameters: (1) the transport of particles to fluids that depends on the nitrogen flow rate and (2) the interparticle transport that depends on the number of particle layers in the sample holder. The nitrogen flow affects the residence time of the vapor phase

https://doi.org/10.1021/acsomega.1c06345
ACS Omega 2022, 7, 16298−16305

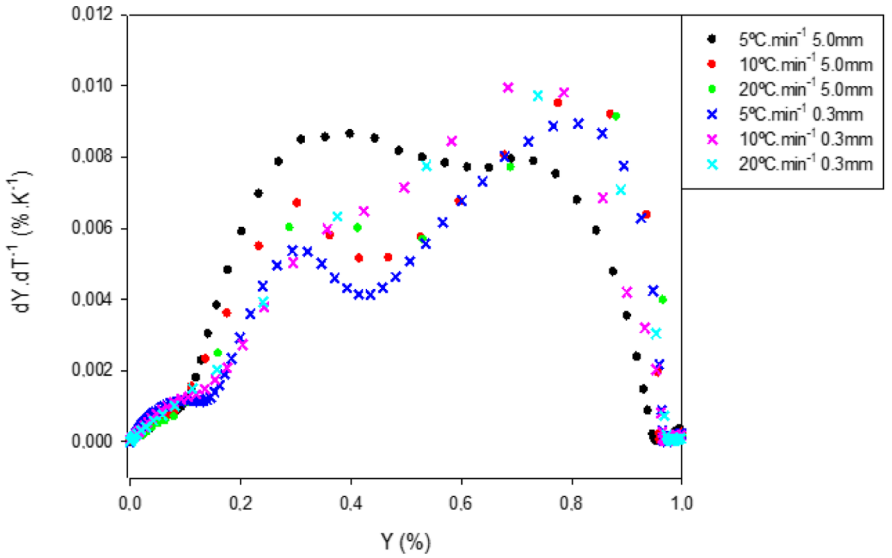

Figure 3. Variation of advanced grade (Y) as a function of $dY{\cdot}dT^{-1}$ for the two-particle sizes of the waste tire (0.3 and 5.0 mm) at three different heating rates applying the Friedman model.

produced by pyrolysis. Additionally, fast flow rapidly removes products from the reaction zone, thereby minimizing side reactions such as cracking and char formation. Regarding the heating rate, it is observed that there is a shift toward the right side, where an increase in the maximum temperature of the decomposition product is evident. This suggests that rapid heating (20 °C min^{-1}) allocates less energy to product formation, so increasing the heating rate favors the formation of products. The mass loss ranges mentioned above are evidenced in the DTG curves for the two-particle sizes (Figures 1B and 2B). The first zone has a maximum peak of 380 °C and the second zone has a maximum of 470 °C. The first stage is associated with 67% w w^{-1} volatile formation due to the volatilization of plasticizers and degradation of NR,[19] and the second zone with 33% w w^{-1} to obtain carbon black from the degradation of the synthetic rubber (styrene-butadiene).[19] These two decomposition zones are more marked for a particle size of 5.0 mm (Figure 2B) and a fusion peak is evident as the heating rate increases. Despite this phenomenon, the performance is neither affected by the heating rate nor by the particle size. The difference between these two zones concerning the heating rate is attributed to heat transfer combined at different heating rates and kinetic decomposition, resulting in delayed corrosion. Additionally, it can be noted that the pyrolysis process is completed when the temperature almost reaches 550 °C, where there is practically no additional weight. Furthermore, in the DTG profile (Figure 1B), the main devolatilization peak occurs at high temperatures and a small peak (shoulder) at low temperatures. These are observed at a low heating rate of 5 °C min^{-1}. The main peak rises as the heating rate increases, and the shoulder disappears. This can be attributed to eliminating side reactions at higher heating rates, increasing devolatilization. In the case of Figure 2B, the devolatilization process is not favored by the particle size because it affects mass transport.

For Miranda et al.,[19] the decomposition of rubber consists of three zones: (1) 120−320 °C with a maximum of 256 °C, (2) 280−440 °C with a maximum of 380 °C, and (3) 400−520 °C with a maximum of 470 °C, which is associated with losses of 33% p p^{-1} residual solid weight and 67% loss due to volatiles. On the other hand, Betancur et al.[32] also define three decomposition zones: (1) 100−270, (2) 270−350, and (3) 350−450 °C, where the first zone is associated with humidity and degradation of additives, the second with the decomposition of NR, and the last with the decomposition of butadiene−styrene by breaking the S−S bonds. In addition, the pyrolysis process is essentially complete above 550 °C, after which no significant mass loss is evident.

Heat-transfer processes, pyrolysis reactions, and mass transfer are fundamental to the pyrolysis process in a tire particle. The process in the tire particle can be described by three zones: virgin tire (internal), reaction zone, and carbon black (external). At the beginning of the process, as seen in Figures 1 and 2, the particle is heated by an external heat flux < 200 °C. Once the surface layer gets hot enough, the particle pyrolyzes at 200−550 °C. By increasing the temperature, the heat propagates toward the center of the particle. With this process, the pyrolysis reactions develop more profound in the particle (virgin zone), and a large amount of volatiles greater than 60% are produced. The tire material becomes fluid due to the accumulation of liquid pyrolysis products in the particle, which causes viscosity in these fluids. The viscosity generates a high resistance to molecular diffusion and intraparticle mass transfer.

Additionally, because the liquid is very viscous, the diffusion of vapor inside the liquid is complex, which results in an accumulation of vapors as vapor bubbles in the particle. As the temperature increases further, the bubbles keep growing and finally, when the bubble's expansion reaches the surface of the liquid, they break and release the contained vapors.

The kinetic process is affected by the volatilization of the elastomers and, in general, by the global degradation of the tire residue. Moreover, the temperature and heating rate plays an essential role in this process. Additional complications may arise when the sample size is above 1.0 mm (Figure 2A) due to mass-transfer phenomena. However, supposing that internal heat transfer is slow, there could be a significant temperature gradient within the particle. In that case, and while using a heating rate of 5 °C min^{-1}, all chemical reactions: pyrolysis, product evaporation, and transport of volatile materials will

https://doi.org/10.1021/acsomega.1c06345
ACS Omega 2022, 7, 16298−16305

occur in a very narrow zone. Thereby, an increase in the endpoint of pyrolysis can be observed at a higher heating rate.

Friedman Differential Method. The Y factor is determined to establish this method, and Figure 3 is made using $dY{\cdot}dT^{-1}$ factor. In this Figure 3, the interval of advanced grade (Y) is chosen according to where the kinetic parameters will be determined. This range must have an adequate linear adjustment. In Figure 3, $dY{\cdot}dT^{-1}$ versus Y, is analyzed, the advanced grade is the interval before the maximum point of the Gaussian distribution to the behavior of the linear range. The kinetic parameters are determined once the Gaussian distribution is determined in each zone. Where to graph $\mathrm{Ln}(dY{\cdot}dT)^{-1}$ versus $(1{\cdot}T^{-1})$, according to eq 6, the activation energy is obtained from the slope. Subsequently by another linearization $[\mathrm{Ln}(dY{\cdot}dT^{-1}) + E_a{\cdot}R^{-1}{\cdot}T]$ versus $\mathrm{Ln}(1 - Y)$, eq 7, the reaction order, and the pre-exponential factor are obtained, as shown in Table 1.

The linear range was chosen for each heating rate using the Friedman method to determine the kinetic parameters (Table 2). The activation energy is between 40.32 and 116.8 kJ mol^{-1}

Table 2. Determination of the Kinetic Parameters at Two Different Rubber Particle Sizes Using the Friedman Differential Method

zone (°C min^{-1})	E_a (kJ mol^{-1})	r^2	A (min^{-1})	n	r^2
Particle Size (0.3 mm)					
5 I	116.8	0.99	1.18×10^8	0.998	0.98
5 II	71.09	0.99	1.66×10^8	0.926	0.98
10	54.07	0.98	1.07×10^4	0.959	0.99
20	40.32	0.99	1.71×10^2	0.937	0.99
Particle Size (5.0 mm)					
5 I	119.1	0.99	5.96×10^8	0.994	0.97
5 II	23.0	1.00	1.03×10^8	3×10^{-12}	0.98
10 I	121.8	0.99	3.27×10^8	0.959	0.96
10 II	69.6	0.99	9.07×10^4	0.817	0.91
20 I	133.0	0.99	3.03×10^9	0.953	1.00
20 II	49.8	0.98	4.73×10^8	1.275	1.00

in the case of the particle size of 0.3 mm and for the one of 5.0 mm the range is between 23.0 and 119.1 kJ mol^{-1}. Comparing the activation energies for the same heating rate at different particle sizes evidences a growth in energy; this may be due to heat transfer effects because the matter does not have enough time to heat evenly. The reaction orders are approximately 1 for all the decomposition zones. The pre-exponential factor in particle size of 5.0 mm is more significant than one of a size of 0.3 mm. Additionally, for the same heating rate at different particle sizes, more than one decomposition product is generated, as in the case of a heating rate of 10 and 20 °C min^{-1}, and said behavior is not maintained using a heating rate of 5 °C min^{-1}. This due to heat transfer phenomena causing parallel decomposition reactions. This variation between the energies of activation proves that a single-stage does not give the decomposition of rubber. However, those products that lead to other reactions in parallel or series are being created.[33]

In the Coats−Redfern method Table 3, increasing the heating rate and particle size, there is a rise in the activation energy due to mass transfer. In rapid heating, there are drastic changes in the material that generates collateral reactions to the decomposition of this material. In addition, the largest activation of energy occurs when a higher heating rate is

Table 3. Determination of Kinetic Parameters Using the Integral Coats−Redfern Method

	E_a (kJ mol^{-1})	r^2
Particle Size (0.3 mm)		
5 I	45.68	0.98
5 II	59.03	0.99
10	80.33	0.99
20	87.85	0.99
Particle Size (5.0 mm)		
5 I	72.50	0.99
5 II	71.63	1.00
10 I	63.50	0.97
10 II	82.76	0.99
20 I	124.58	0.99
20 II	43.58	0.98

applied and this indicates that at a higher heating rate, there is a delay in the degradation of the rubber. It should be noted that the Coats−Redfern method requires that the work be done at the beginning of the reaction, and there is no significant change in the reaction mechanism of the material for the different degradation ranges.[26]

Comparing the Friedman and Coats methods for the same heating rate and the same linearity range, it is found that at a heating rate of 5 °C min^{-1} decreases the activation energy, while for speeding, greater than five increases the activation energy. This can be associated with the fact that a high variation in the heating rate affects the degradation range of the rubber, and it affects the moment when the kinetic models are applied since the degradation mechanism is not constant for the entire degradation range. Despite this, the activation energies in the two methods are between the same ranges and are like those reported in previous studies.[18,20,34]

Finally, the standard test method for decomposition kinetics by thermogravimetry, ASTM E1641, is applied, and the results are reported in Tables S1−S4, 4, and 5. According to the

Table 4. Determination of $E_a{\cdot}(RT)^{-1}$ for the Two Particle Sizes according to ASTM E1641

	5 °C min^{-1}	10 °C min^{-1}	20 °C min^{-1}	average
Particle Size (0.3 mm)				
E_a (J mol^{-1})	64 622	64 622	64 622	64 622
R (J mol^{-1} K^{-1})	8.314	8.314	8.314	
T (K)	521	546	560	
$E_a(RT)^{-1}$ (J mol^{-1} K^{-1})	14.91	14.23	13.88	14.34
Particle Size (5.0 mm)				
E_a (J mol^{-1})	61 615	61 615	61 615	61 615
R (J mol^{-1} K^{-1})	8.314	8.314	8.314	
T (K)	537	571	576	
$E_a(RT)^{-1}$ (J mol^{-1} K^{-1})	13.80	12.98	12.86	13.21

standard, the value of $E_a(RT_c)^{-1}$, T_c is the temperature at the constant conversion for the heating rate closest to the midpoint of the experimental heating rates. The standard test recommends taking this temperature at 95% weight loss seen in Table S1. After linearization, the energy of estimated activation without integration is shown in Table S2.

With the activation energy estimated according to the standard, $E_a(RT_c)^{-1}$ (Table 4) was determined, and from this

https://doi.org/10.1021/acsomega.1c06345
ACS Omega 2022, 7, 16298−16305

Table 5. Results of the Kinetic Study Using the ASTM E1641 Standard for Two Particle Sizes of Waste Tire

	0.3 mm			5.0 mm		
β (°C min^{-1})	E_a (kJ mol^{-1})	A (min^{-1})	K (min^{-1})	E_a (kJ mol^{-1})	A (min^{-1})	K (min^{-1})
5	60.1	26 672	0.02515	56.9	7957	0.01565
10	59.9	24 742	0.04651	56.3	6313	0.02603
20	59.7	33 171	0.08914	56.2	11124	0.03508

value, the numerical integration constants, the true b' and a, and then interpolating with help from Table S3 presented in the standard and together at Table S4 the true values a and b are obtained in Table S4, and with them accordingly to ASTM E1641 the activation energy reported in Table 5.

Using the ASTM E1641 standard for a decomposition value of 95% at all heating rates, it is observed that increasing the heating rate decreases the activation energy and increases the reaction rate constant (K). According to the Arrhenius equation, the temperature rise produces an increase in the rate constant and with it, a greater reaction rate. The activation energies are between a range between 56 and 60 kJ mol^{-1}, the value that is close to previous studies of waste tire decomposition. Miranda et al. find activation energies between 34 and 178 kJ mol^{-1} and Singh et al. 80 kJ mol^{-1} a 99 kJ mol^{-1}. It can therefore be concluded that the variation in activation energies may be due to the amount of initial mass and the method used to determine the kinetics parameters, which depends on the approximations used to determine them. In addition to the type of tire that the researchers use for the study because there is a variation in its composition.

Additionally, it is important to highlight that the ASTM E1641 standard is only considered in a 95% decomposition stage, paying no heed to intermediary decomposition, as is the case of styrene-butadiene or butadiene.[35]

Finally, when comparing the values obtained in the kinetic parameters for the pyrolysis of waste tires, it is evidenced that there is a variation between the three methods due to many reactions in parallel and series. It is only by TGA that weight loss can be measured generally due to these reactions, depending on the range of decomposition in which each method is pertinent to be applied. However, the methods are useful for providing comparative kinetics with data in different reaction conditions, such as temperature and heating rate, to elucidate the conditions helpful in an industrial pyrolysis process. Additionally, suppose a comparison of the results obtained from the activation energy and collision factor is made. In that case, it is found that there are significant differences in the values because each study method uses different fundamentals, and different approaches are used how the differential, integral, or ASTM E1641 standard at 95% decomposition.

CONCLUSIONS

To sum up, the pyrolysis process of waste tires has two thermal decomposition stages in the range between 200 and 520 °C, which corresponds to the volatilization of plasticizers and the degradation of natural and synthetic rubber. Besides, it was found that when the heating rate increases, the temperature ranges where decomposition occurs increase. By TGA of the pyrolysis of waste tires, kinetic parameters, such as the activation energy, the pre-exponential factor, the kinetic constant, and the reaction order, were determined.

The above-mentioned parameters were determined by three different methods. The values of activation energy, which depends on the heating rate, obtained are as follows: by the differential method, in the range of 23 to 119 kJ mol^{-1}; by the integral method, from 43 to 124 kJ mol^{-1}; and, finally, by the ASTM E1641 method, from 56 to 60 kJ mol^{-1}. The pre-exponential factor was lower when using the ASTM E1641 standard compared to those of the integral and differential methods. Ultimately, the approximate reaction order was 1 in each decomposition zone. Depending on the mathematical method used, different values were obtained for the kinetic parameters due to the approximations used by each method. Another conclusion of this research was that the particle size strongly influences the degradation kinetics by influencing mass transport. At a larger size, higher values were obtained for all kinetic parameters where the processes of heat and mass transfer affect the overall degradation rate of the material.

ASSOCIATED CONTENT

Supporting Information

The Supporting Information is available free of charge at https://pubs.acs.org/doi/10.1021/acsomega.1c06345.

Parameters obtained by applying the ASTM E1641 standard (PDF)

AUTHOR INFORMATION

Corresponding Author

Juan Carlos Moreno-Piraján − *Departamento de Química, Grupo de Investigación en Sólidos Porosos y Calorimetría, Facultad de Ciencias, Universidad de los Andes, Bogotá 111711, Colombia;* orcid.org/0000-0001-9880-4696; Phone: +57(1) 3394949ext3465; Email: jumoreno@uniandes.edu.co

Authors

Aida M. Ramírez Arias − *Departamento de Química, Grupo de Investigación en Sólidos Porosos y Calorimetría, Facultad de Ciencias, Universidad de los Andes, Bogotá 111711, Colombia*

Liliana Giraldo − *Departamento de Química, Facultad de Ciencias, Universidad Nacional de Colombia, Bogotá 111321, Colombia*

Complete contact information is available at: https://pubs.acs.org/10.1021/acsomega.1c06345

Notes

The authors declare no competing financial interest.

ACKNOWLEDGMENTS

The authors thank the Research and Postgraduate Committee-Faculty of Sciences of the Universidad de Los Andes, Colombia. The authors also thank the framework agreement between Universidad Nacional de Colombia and Universidad de Los Andes (Bogotá, Colombia) under which this work was carried out. The J.C.M.-P.á also thanks for the award from the Facultad de Ciencias of Universidad de los Andes, number

INV-2021-128-2257, and the support of "Publica tus Nuevos Conocimientos y Expón tu Nuevas Creaciones", de la Vicerrectoría de investigaciones de la Universidad de los Andes (Bogotá, Colombia).

REFERENCES

(1) ETRMA 2019. http://www.etrma.org/media-centre/press-releases (accessed on January 15, 2022).
(2) Miranda, R. C.; Segovia, C. C.; Sosa, C. A. Pirólisis de Llantas Usadas: Estudio Cinético e Influencia de Variables de Operación. *Inf. Tecnol.* **2006**, *17*, 7−14.
(3) Day, K. E.; Holtze, K. E.; Metcalfe-Smith, J. L.; Bishop, C. T.; Dutka, B. J. Toxicity of leachate from automobile tires to aquatic biota. *Chemosphere* **1993**, *27*, 665−675.
(4) López, G.; Olazar, M.; Aguado, R.; Bilbao, J. Continuous pyrolysis of waste tyres in a conical spouted bed reactor. *Fuel* **2010**, *89*, 1946−1952.
(5) Lemieux, P.; Ryan, J. V. Characterization of air pollutants emitted from a simulated scrap tire fire. *J. Air Waste Manage. Assoc.* **1993**, *43*, 116−1115.
(6) Lou, J. C.; Lee, G. F.; Chen, K. S. Incineration of styrene-butadiene rubber: the influence of heating rate and oxygen content on gas products formation. *J. Hazard. Mater.* **1998**, *58*, 165−178.
(7) Hashem, F. S.; Razek, T. A.; Mashout, H. A. Rubber and plastic wastes as alternative refused fuel in cement industry. *Constr. Build. Mater.* **2019**, *212*, 275−282.
(8) Choi, G.-G.; Jung, S.-H.; Oh, S.-J.; Kim, J.-S. Total utilization of waste tire rubber through pyrolysis to obtain oils and CO_2 activation of pyrolysis char. *Fuel Process. Technol.* **2014**, *123*, 57−64.
(9) Garcia-Perez, M.; Wang, X. S.; Shen, J.; Rhodes, M. J.; Tian, F.; Lee, W.-J.; Wu, H.; Li, C.-Z. Fast Pyrolysis of Oil Mallee Woody Biomass: Effect of Temperature on the Yield and Quality of Pyrolysis Products. *Ind. Eng. Chem. Res.* **2008**, *47*, 1846−1854.
(10) Ramirez-Canon, A.; Muñoz-Camelo, Y.; Singh, P. Decomposition of Used Tyre Rubber by Pyrolysis: Enhancement of the Physical Properties of the Liquid Fraction Using a Hydrogen Stream. *Environments* **2018**, *5*, 72.
(11) Leung, D. Y. C.; Yin, X. L.; Zhao, Z. L.; Xu, B. Y.; Chen, Y. Pyrolysis of tire powder: influence of operation variables on the composition and yields of gaseous product. *Fuel Process. Technol.* **2002**, *79*, 141−155.
(12) Conesa, J. A.; Fullana, A.; Font, R. Tire pyrolysis: Evolution of Volatile and Semi-volatile Compounds. *Energy Fuels* **2000**, *14*, 409−418.
(13) González, J. F.; Encinar, J. M.; Canito, J. L.; Rodríguez, J. J. Pyrolysis of automobile tyre Waste. Influence of operating variables and kinetics study. *J. Anal. Appl. Pyrolysis* **2001**, *58*−*59*, 667−683.
(14) Aranzazu Rios, L. M.; Cárdenas, P.; Cárdenas, J.; Gaviria, G.; Rojas, A. Kinetic Models of Polymer Thermal Decomposition: a review. *Rev. Ing. Univ. Medellin* **2013**, *12*, 113.
(15) Boukadir, D.; David, J.-C.; Granger, R.; Vergnaud, J.-M. Preparation of a convenient filler for thermoplastics by pyrolysis of rubber powder recovered from tyres. *J. Anal. Appl. Pyrolysis* **1981**, *3*, 83−89.
(16) Bouvier, J. M.; Charbel, F.; Gelus, M. Gas-solid pyrolysis of tire wastes- Kinetics and material balances of batch pyrolysis of used tires. *Resour. Conserv.* **1987**, *15*, 205−214.
(17) Mui, E. L. K.; Cheung, W. H.; Mckay, G. Tyre char preparation from waste tyre rubber for dye removal from effluents. *J. Hazard. Mater.* **2010**, *175*, 151−158.
(18) Kim, S.; Park, J. K.; Chun, H.-D. Pyrolysis kinetics of scrap tire rubbers I: Using DTG and TGA. *J. Environ. Eng.* **1995**, *121*, 507−514.
(19) Miranda, M.; Pinto, F.; Gulyurtlu, I.; Cabrita, I. Pyrolysis of rubber tyre wastes: a kinetic study. *Fuel* **2013**, *103*, 542−552.
(20) Leung, D. Y. C.; Wang, C. L. Kinetic modeling of scrap tire pyrolysis. *Energy Fuels* **1999**, *13*, 421−427.
(21) Yaxin, S.; Bingtao, Z. Pyrolysis of waste tire and its model. Bioinformatics and biomedical engineering. *4th International Conference*, 2010.
(22) Qu, B.; Li, A.; Qu, Y.; Wang, T.; Zhang, Y.; Wang, X.; Gao, Y.; Fu, W.; Ji, G. Kinetic analysis of waste tire pyrolysis with metal oxide and zeolitic catalysts. *J. Anal. Appl. Pyrolysis* **2020**, *152*, 104949.
(23) Mkhize, N. M.; Danon, B.; Van der Gryp, P.; Görgens, J. F. Kinetic study of the effect of the heating rate on the waste tyre pyrolysis to maximise limonene production. *Chem. Eng. Res. Des.* **2019**, *152*, 363−371.
(24) Menares, T.; Herrera, J.; Romero, R.; Osorio, P.; Arteaga-Pérez, L. E. Waste tires pyrolysis kinetics and reaction mechanisms explained by TGA and Py-GC/MS under kinetically-controlled regime. *J. Waste Manage.* **2020**, *102*, 21−29.
(25) Friedman, H. L. Kinetics of thermal degradation of char-forming plastics from thermogravimetry. Application to a phenolic plastic. *J. Polym. Sci., Part C: Polym. Symp.* **1964**, *6*, 183.
(26) Coats, A. W.; Redfern, J. P. Kinetic parameters from thermogravimetric data. II. *J. Polym. Sci., Polym. Phys. Ed.* **1965**, *3*, 917−920.
(27) Masel, R. *Principles of Adsorption and Reaction on Solid Surfaces*; University of Illinois at Urbana Champaign: Illinois, 1951.
(28) Aylón, E.; Callén, M. S.; López, J. M.; Mastral, A. M.; Murillo, R.; Navarro, M. V. Assessment of tire devolatilization kinetics. *J. Anal. Appl. Pyrolysis* **2005**, *74*, 259−264.
(29) Williams, P. T.; Besler, S. Pyrolysis-thermogravimetric analysis of tyres and tyre components. *Fuel* **1995**, *74*, 1277−1283.
(30) Teng, H.; Serio, M. A.; Wojtowicz, M. A.; Bassilakis, R.; Solomon, P. R. Reprocessing of used tires into activated carbon and other products. *Ind. Eng. Chem. Res.* **1995**, *34*, 3102−3111.
(31) Senneca, O.; Chirone, R.; Salatino, P. A Thermogravimetric Study of Nonfossil Solid Fuels. 2. Oxidative Pyrolysis and Char Combustion. *Energy Fuels* **2002**, *16*, 661−668.
(32) Betancur, M.; Martínez, J. D.; Murillo, R. Production of activated carbon by waste tire thermochemical degradation with CO_2. *J. Hazard. Mater.* **2009**, *168*, 882−887.
(33) Brazier, D. W.; Schwartz, N. V.; Schwartz, D. The effect of heating rate on the thermal degradation of polybutadiene. *J. Appl. Polym.* **1978**, *22*, 113−124.
(34) Conesa, J. A.; Font, R.; Marcilla, A. Mass spectrometry validation of a kinetic model for the thermal decomposition of tyre wastes. *J. Anal. Appl. Pyrolysis* **1997**, *43*, 83−96.
(35) Singh, S.; Wu, C.; Williams, P. T. Pyrolysis of waste materials using TGA-MS and TGA-FTIR as complementary characterisation techniques. *J. Anal. Appl. Pyrolysis* **2012**, *94*, 99−107.

https://doi.org/10.1021/acsomega.1c06345
ACS Omega 2022, 7, 16298−16305